Comparative studies of electronic structures of sodium metasilicate and α and β phases of sodium disilicate

W. Y. Ching and R. A. Murray
Department of Physics, University of Missouri—Kansas City, Kansas City, Missouri 64110

D. J. Lam and B. W. Veal
Materials Science and Technology Division, Argonne National Laboratory, Argonne, Illinois 60439

(Received 18 March 1983)

The electronic structures of sodium metasilicate (Na_2SiO_3) and the α and β phases of sodium disilicate ($Na_2Si_2O_5$) are calculated from first principles by the method of linear combination of atomic orbitals. Two different sets of calculations with exchange parameter α set equal to $\frac{2}{3}$ and 1.0 were performed. Results are presented in terms of total and partial density of states and the valence electron charge distribution. The calculated electronic structures are discussed in connection with the local structural environment of each type of atom in these crystals. Comparison with experimental x-ray photoelectron spectra on $(Na_2O)_x(SiO_2)_{1-x}$ glasses suggests that local short-range order in crystalline and glassy alkali silicates is similar.

I. INTRODUCTION

Although the science of silicate glasses has been studied since ancient times, research work on silicate glasses at the microscopic level has been relatively recent. In recent years, technological applications of glasses ranging from high-quality optical fibers to host materials for radioactive waste storage have stimulated detailed investigations on the structure and properties of various silicate glasses.[1] Of particular interest are alkali silicate glasses which can be formed in a wide range of compositions by dissolving controlled amounts of alkali oxide in silicon dioxide. In such glasses, the SiO_4 tetrahedral unit is still maintained as the structural backbone, but the exact local environment of the alkali ions is less certain. Based on chemical considerations, it has been generally accepted[2] that a monovalent alkali oxide such as sodium oxide (Na_2O) enters the SiO_2 glass network by breaking an SiO bond and creating two nonbridging oxygens (NBO) with a Na^+ ion located close to the NBO for charge compensation. Such a description appears to be valid at low alkali concentrations. However, if the composition of Na_2O becomes appreciable, the situation can be much more complicated. Furthermore, the exact geometries near the NBO and Na^+ ions are not known. Fortunately there occurs in nature a large class of complex mineral crystalline forms of alkali silicate. The structures of many of these crystals have been determined. These crystals represent thermodynamical stable phases containing fixed ratios of alkali oxides and silica. It is logical to study these complicated crystal forms with well-determined structural parameters in order to shed some light on the less understood $(R_2O)_x(SiO_2)_{1-x}$ glass systems, where R denotes a monovalent alkali-metal element.

In this paper we calculate the electronic structure of three crystalline forms; i.e., sodium metasilicate (Na_2SiO_3) and two forms of sodium disilicate (α-$Na_2Si_2O_5$ and β-Na_2SiO_5). The calculations are compared with experimental x-ray photoelectron spectroscopy (XPS) results on crystalline and glassy silicates. In this way, relevant information about the atomic structures and the electronic states of silicate glass may be obtained.

In the next section we analyze the structures of the three silicate crystals. The method for performing the electronic structure calculations is briefly outlined in Sec. III. The results are discussed in Sec. IV where comparison with experiments is also made. The last section is devoted to some concluding remarks.

II. ATOMIC ARRANGEMENT

A. Sodium metasilicate (Na_2SiO_3)

The crystal lattice is orthorhombic with 24 atoms in the unit cell and the space group is $Cmc2_1$.[3] The structure was reevaluated by McDonald and Cruickshank[3] and their lattice parameters were used in the present calculation. Figure 1 shows schematically how each type of atom is related to the others. There are two types of O atoms in this structure. Each of the bridging oxygen (BO) atoms [O_2 in Fig. 1] is bonded to two Si atoms thereby joining the SiO_4 tetrahedra. This bonding arrangement results in the formation of chains (of tetrahedra) parallel to the c axis. The NBO atoms (O_1 in Fig. 1) bond to only one Si atom, and do not participate in the chain-forming structure. The mean Si-O distance is 1.632 Å. This is a typical bond distance in the SiO_4 tetrahedra (α quartz, for example has a mean Si—O bond length of 1.610 Å). The bond length (BL) varies substantially in Na_2SiO_3 (as well as in α and β sodium disilicates) depending on the type of O sites involved. The NBO Si—O BL is 1.592 Å, while for the BO atoms the Si—O bond lengths are 1.677 and 1.668 Å. This variation in BL results in distortion of the SiO_4 units. The O—Si—O angles range from 103.06° to 116.89° with

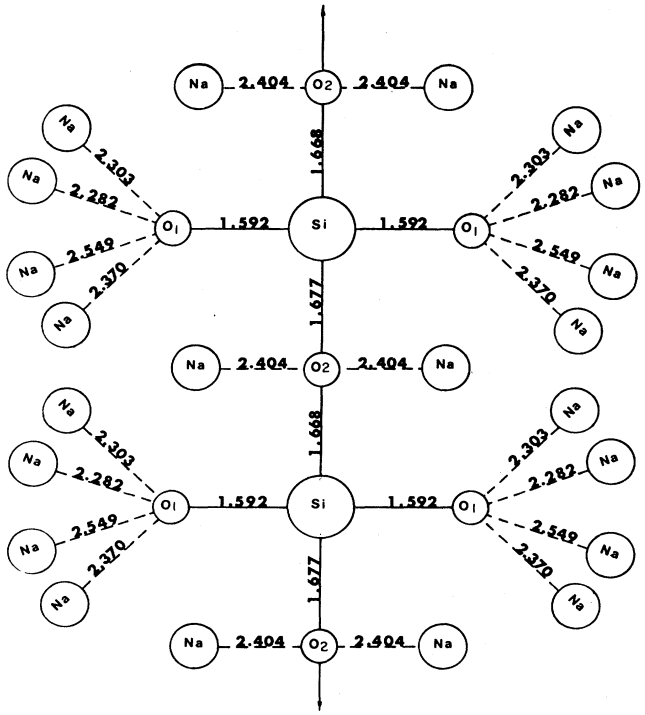

FIG. 1. Schematic drawing of the bonding relationship in Na_2SiO_3; O_1 is the nonbridging O and O_2 is the bridging O. Units are Å.

an average of 109.46°.[3] The NBO atoms are surrounded by four Na atoms at distances of 2.282—2.549 Å. This fourfold coordination of the NBO atoms to Na is common to all three crystals studied. In Na_2SiO_3 the Na atoms serve to separate the metasilicate chains in the $\vec{a}$ and $\vec{b}$ directions. The separation is sufficiently great to form fairly large empty channels parallel to the chains. It is not clear if such features also exist in the glasses. An interesting feature of this structure is that even though the BO atoms are each bonded to two Si atoms, they are also close to two Na atoms, both at 2.404 Å. This distance is comparable to the Na—O bond lengths for the NBO atoms. Judging from the Na-O nearest-neighbor separations it would appear that the sodium atoms are not strongly bonded to any particular atom.

B. Alpha sodium disilicate (α-$Na_2Si_2O_5$)

The α-$Na_2Si_2O_5$ is orthorhombic with a space group of *Pncb*. There are 36 atoms in the unit cell. The most recent lattice parameters and fractional coordinates were determined by Pant and Cruickshank.[4] Figure 2 shows the schematic bonding relationships of the atoms in α-$Na_2Si_2O_5$. The structure is similar to Na_2SiO_3, but now each Si atom bonds to three BO atoms and one NBO atom. Relative to Na_2SiO_3, an extra BO occurs that links the chains of SiO_4 tetrahedra into sheets running parallel to the (010) plane. Gaps in these sheets are aligned so that channels are formed in the $\vec{c}$ direction. Two types of BO are identified; one BO (O_2) is coordinated to one Na atom (O-Na distance 2.386 Å) and the other BO(O_1) has no Na atoms within 3 Å. The same fourfold coordination of Na atoms to the NBO atoms (O_3) is present with the O-Na distances ranging from 2.290—2.600 Å. As in the Na_2SiO_3 case, the Si—O BL is considerably shortened on the nonbridging site but the tetrahedral angles are not as distorted (O—Si—O angles range from 105.42° to 113.20° with an average of 109.42°).[4] The mean Si—O BL is 1.617 Å. This is slightly less than the Si—O BL in Na_2SiO_3.

C. Beta sodium disilicate (β-$Na_2Si_2O_5$)

The β-$Na_2Si_2O_5$ has a monoclinic lattice and the space group is $P2_1/a(C_{2h}^5)$.[5] A reevaluation of the lattice parameters was conducted by Pant.[5] Like α-$Na_2Si_2O_5$, the unit cell contains 36 atoms. The local atomic bonding configurations are shown schematically in Fig. 3. Even though the symmetry and lattices are different, the local structure of α- and β-$Na_2Si_2O_5$ are remarkably similar. Comparing Figs. 2 and 3, one can see that most of the relationships are roughly the same. There are subtle differences, however. Like the α phase, there are metasilicate-like chains which are linked to form sheets separated by the Na atoms. But in this case the channels run parallel to the *b* axis. Unlike the α phase, the chains are not identical so there are two unique positions for the silicon atoms with slightly different BL and BA. Consequently, there are two nonequivalent Na positions and two different NBO positions (O_4 and O_5). As mentioned earlier, the NBO sites have shorter Si—O BL than BO sites. The range of O—Si—O angle values (104.96° to 115.94° with an average of 109.38°) (Ref. 5) is slightly less than that of Na_2SiO_3 and slightly greater than that of α-$Na_2Si_2O_5$. The mean Si—O BL is 1.622 Å for Si_1 and 1.626 Å for Si_2. This is less than the Na_2SiO_3 and greater than the α-$Na_2Si_2O_5$. Both NBO atoms have four Na nearest neighbors as mentioned before, but the NBO-Na distances are different. For O_4, the Na distances range from 2.326—2.588 Å and for O_5 the range is from 2.306—2.569 Å. In β-$Na_2Si_2O_5$, all three of the BO atoms (O_1, O_2, O_3) are close to a single Na atom with Na-O distances of 2.425, 2.482, and 2.495 Å, respectively.

Referring to Table I, we summarize several observations regarding systematic behavior in the crystal structures of binary alkali silicates:

(1) The SiO_4 tetrahedron distorts when nonbridging oxygen atoms are introduced into the tetrahedron,

(2) the NBO—Si bond length is always less than the BO—Si bond length, and

(3) as more NBO's are added to a SiO_4 tetrahedron, the distance between the Si and the remaining BO's increases. The average NBO-Si distance remains relatively fixed.

These microscopic characteristics of crystalline silicates may provide useful guidelines for modeling amorphous silicates where similar considerations may be expected to prevail.

III. METHODS OF CALCULATION

The electronic structures of the three sodium silicate crystals were calculated using a direct-space first-principles orthogonalized linear combination of atomic orbitals (OLCAO) method.[6] This is an extension of the more conventional linear combination of atomic orbitals (LCAO) method.[7] Since no experimental data on the single-crystal silicates exist, our major aim would be to obtain the density of states (DOS) curves for the crystalline silicates and to make comparisons with the experimental results on silicate glasses and polycrystalline silicates.[2] Accordingly, no laborious self-consistent field calculations were attempted and only a minimal basis set for each atom was employed. It has been shown that such calculations are able to give realistic electronic structures of complex silicon nitride and silicon oxynitride crystals.[8] Since the method is well described in the published literature, only a brief outline is given here. The model potential for each atom was extracted from the superposition of atomic charges appropriate to the Na_2SiO_3 crystal. The exchange potential was built according to the usual local density functional theory.[9] Two sets of calculations were performed, one with the exchange parameter $\alpha=\frac{2}{3}$ and the other with $\alpha=1.0$. In this model the potentials for BO and NBO were different because of the different charge distributions surrounding the two types of O atoms. However, no distinction was made for the same type of atom at nonequivalent sites. The potentials were spherically averaged and the same potential functions were used in the calculations for all three crystals. A single calculation utilizing a Gaussian orbitals basis for each atomic po-

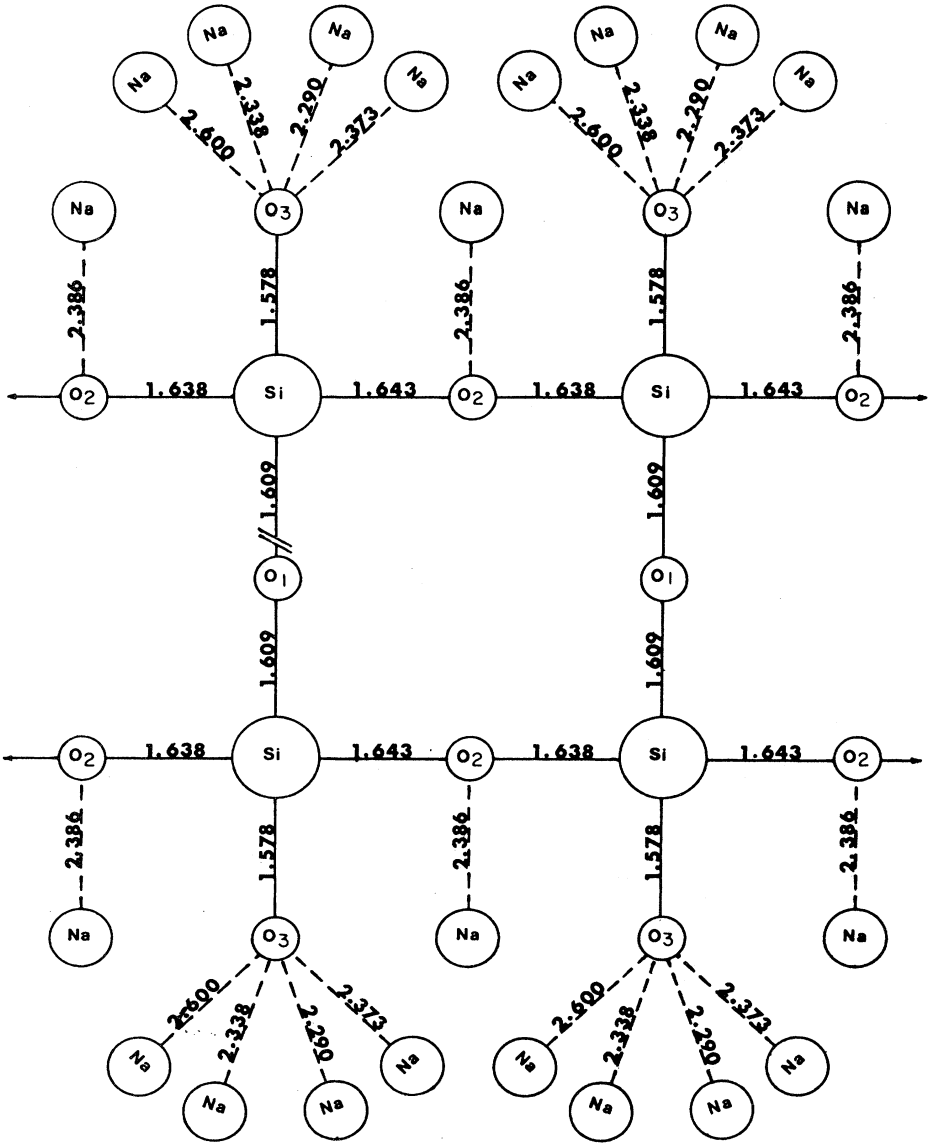

FIG. 2. Schematic drawing of the bonding relationship in α-$Na_2Si_2O_5$. O_1,O_2 are bridging O; O_3 nonbridging O. Units are Å.

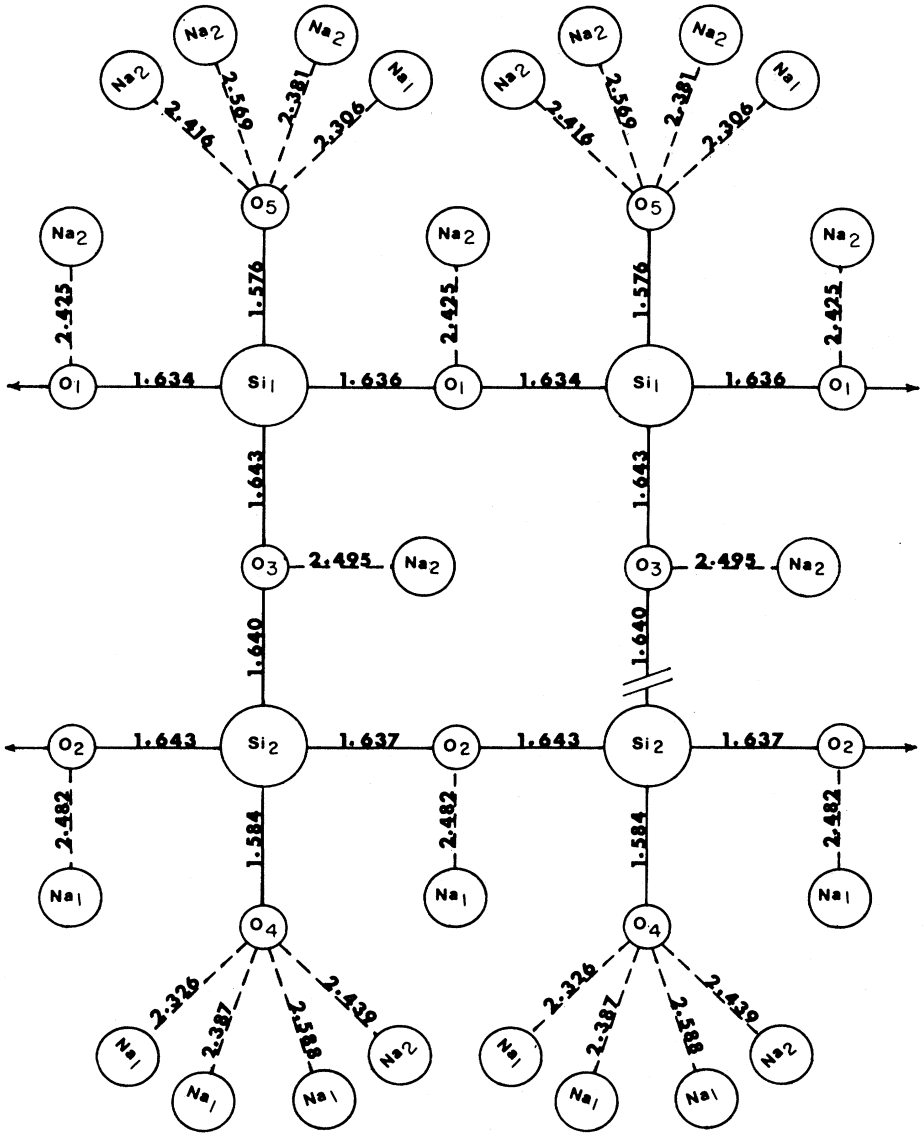

FIG. 3. Schematic drawing of the bonding relationship in β-$Na_2Si_2O_5$. O_1, O_2, O_3 are bridging O; O_4, O_5 are nonbridging O. Units are Å.

tential yielded the contracted atomiclike wave functions which were used as the basis functions for the OLCAO calculations. A minimal basis set of $1s, 2s, 2p_x, 2p_y, 2p_z$, $3s, 3p_x, 3p_y, 3p_z$ for Na and Si atoms and $1s, 2s, 2p_x, 2p_y, 2p_z$ for O atoms was used. After explicitly calculating the overlap and the Hamiltonian integrals, lattice sums were performed to full convergence. The secular equations were then solved at the eight corner $\vec{k}$ points of the irreducible part of the Brillouin zone (BZ). Based on the eigenvalues and eigenvectors at these eight $\vec{k}$ points, the

TABLE I. Bond lengths in silicates

	NBO-tetrahedron	Average BO bond length (Å)	Average NBO bond length (Å)
SiO_2	0	1.610	
α-$Na_2Si_2O_5$	1	1.630	1.578
β-$Na_2Si_2O_5$	1	1.639	1.576
$Na_2Si_2O_3$	2	1.673	1.592

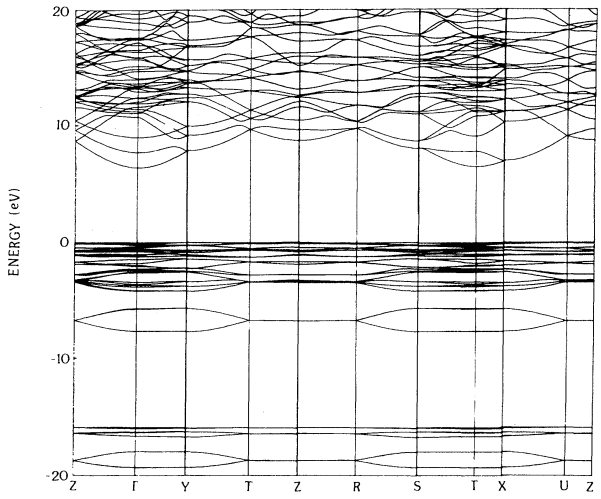

FIG. 4. Band structure of Na_2SiO_3 along the symmetry lines calculated with exchange potential parameter $\alpha=\frac{2}{3}$.

DOS curves were constructed. The partial DOS (PDOS) and the effective charges on each atoms were also calculated with the use of Mulliken's scheme of population analysis.[10]

IV. RESULTS AND DISCUSSION

A. Band structure and density of states

Figure 4 shows the band structure of Na_2SiO_3 along the symmetry lines for the $\alpha=\frac{2}{3}$ calculation. This is a typical silicate band structure and we present it for illustrative purposes. In Table II, we summarize the band gap values for each of the three crystals in the two sets of calculations. These gap values are to be considered as upper limits within their respective potential models since more detailed calculations utilizing self-consistency and extended basis sets would probably reduce these gap values. We found no experimental determinations of energy gaps for single crystals of these silicates. Optical measurements on $(Na_2O)_x(SiO_2)_{1-x}$ glasses[11] indicate that the gap is about 6 eV for $x=0.30$. Since the band gap of amorphous silicon dioxide (α-SiO_2) is about 8.9 eV,[12] addition of Na_2O to the glass tends to reduce the gap value. The $\alpha=\frac{2}{3}$ calculations appear to be in better agreement with these experimental results than the $\alpha=1$ calculations. No other detailed band-structure calculations on these crystals exist. Ellis *et al.*[13] used a simplified LCAO method with parametrized integral values to calculate the band structure of a molecular fragment of sodium disilicate and found a gap of about 8 eV.

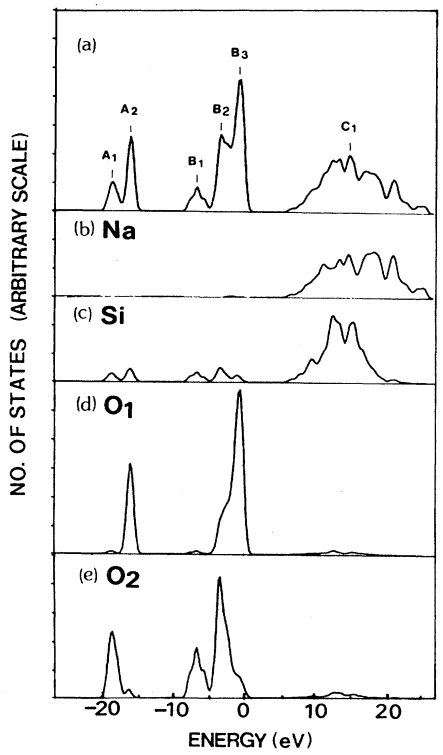

FIG. 5. DOS and PDOS for Na_2SiO_3 calculated with exchange parameter $\alpha=\frac{2}{3}$. The top panel is the total DOS in arbitrary units. The lower panels are the PDOS for each type of atoms indicated and normalized to the number states per atom. (a) Total, (b) Na, (c) Si, (d) NBO (O_1), (e) BO (O_2).

B. Density of states and partial density of states

For each crystal, the DOS and PDOS were obtained from the calculated eigenvalues and eigenvectors. Each energy state was given a small Gaussian broadening of about 0.5 eV. In Figs. 5–7 the DOS curves of Na_2SiO_3, α-$Na_2Si_2O_5$, and β-$Na_2Si_2O_5$ with $\alpha=\frac{2}{3}$ are presented.

TABLE II. Band-structure information.

		$\alpha=\frac{2}{3}$	$\alpha=1.0$
Na_2SiO_3	Band gap (eV)	6.46 (indirect)	9.98 (indirect)
	ΔE_{O2s} (eV)	2.50	2.32
α-$Na_2Si_2O_5$	Band gap (eV)	7.22 (indirect)	8.98 (direct at point Γ)
	ΔE_{O2s} (eV)	1.51	3.19
β-$Na_2Si_2O_5$	Band gap (eV)	6.89 (direct at point Γ)	8.46 (direct at point Γ)
	ΔE_{O2s} (eV)	1.81	3.27

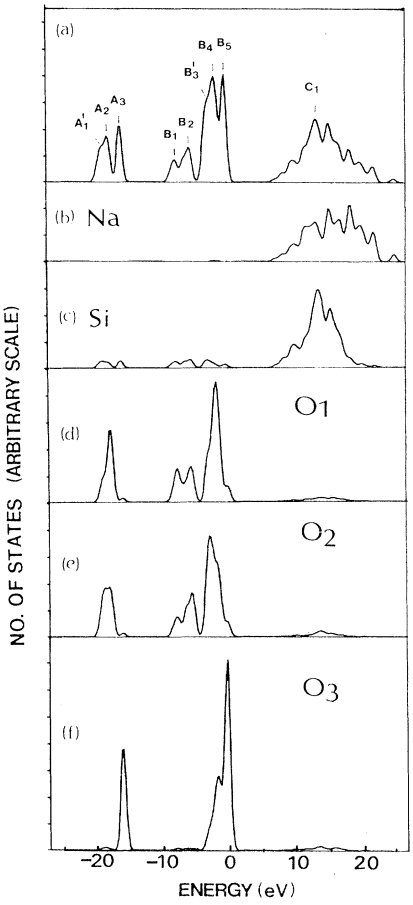

FIG. 6. Same as Fig. 5 for α-$Na_2Si_2O_5$. (a) Total, (b) Na, (c) Si, (d) BO (O_1), (e) BO (O_2), (f) NBO (O_3).

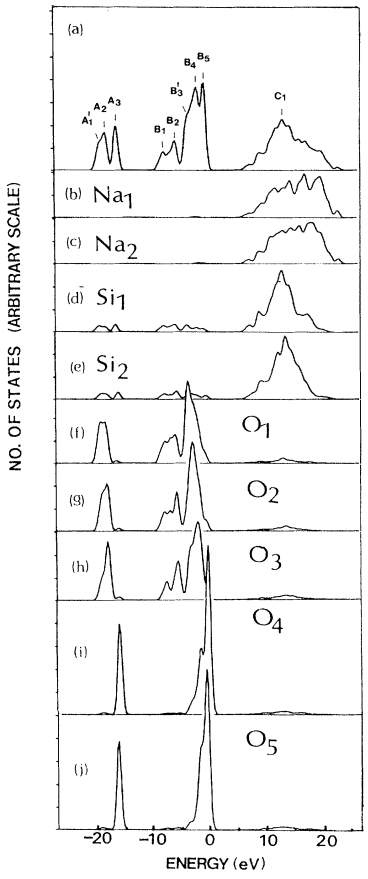

FIG. 7. Same as Fig. 5 for β-$Na_2Si_2O_5$. (a) Total, (b) Na_1, (c) Na_2, (d) Si_1, (e) Si_2, (f) BO (O_1), (g) BO (O_2), (h) BO (O_3, (i) NBO (O_4), (j) NBO (O_5).

The corresponding curves for the $\alpha=1$ calculation are shown in Figs. 8–10. In each figure the top panel represents the total DOS and the lower panels are PDOS projected on each type of atom (scaled according to the proper number of atoms per formula unit). PDOS for atoms of the same type but with nonequivalent positions (as discussed in Sec. II) are also separated. In addition to the different gap values discussed above, the major differences between $\alpha=\frac{2}{3}$ and $\alpha=1$ calculations are as follows: (1) In the $\alpha=1$ case the ionized Na states are higher in energy resulting in a larger gap. In this case the bottom of the conduction band (CB) consists almost exclusively of Si states. With the $\alpha=\frac{2}{3}$ calculation, the bottom of the CB consists of both Na and Si states. (2) The splitting (ΔE) of the O2s peaks resulting from the presence of both BO and NBO is significantly larger in the $\alpha=1$ case than in the $\alpha=\frac{2}{3}$ case for the disilicates; the splitting is comparable for metasilicates. The calculated values ($\Delta E_{O\,2s}$) are listed in Table II. The experimental splitting of the O 2s level determined by fitting the doublet with two Gaussians (each with half width of $\sim$2.5 eV) is 2.5 eV for both the disilicate and the metasilicate. This splitting is close to the mean (of the $\alpha=1$ and $\alpha=\frac{2}{3}$ values) of the calculated O 2s splittings for the compositions listed in Table II and

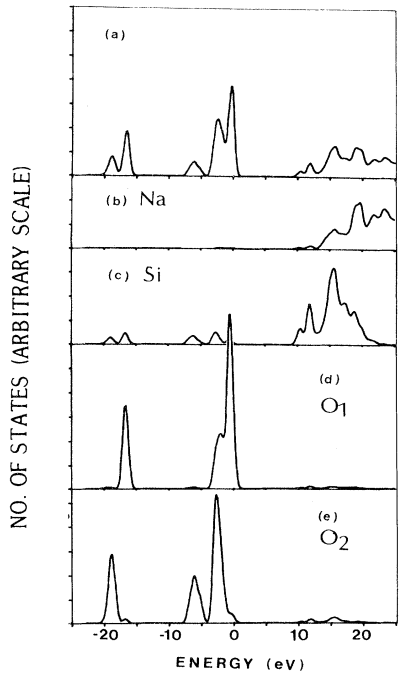

FIG. 8. Same as Fig. 5 for Na_2SiO_3 calculated with exchange parameter $\alpha=1.0$.

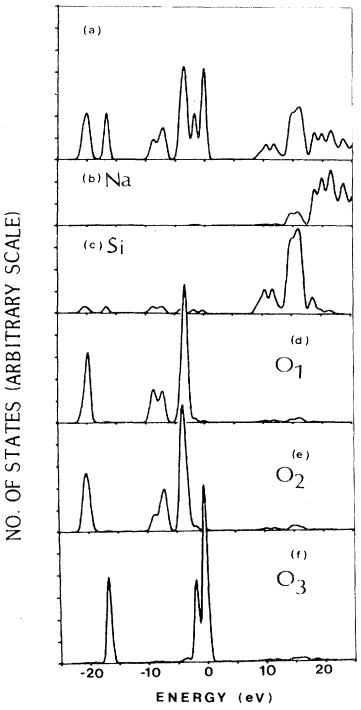

FIG. 9. Same as Fig. 8 for α-$Na_2Si_2O_5$. Calculated with $\alpha=1.0$.

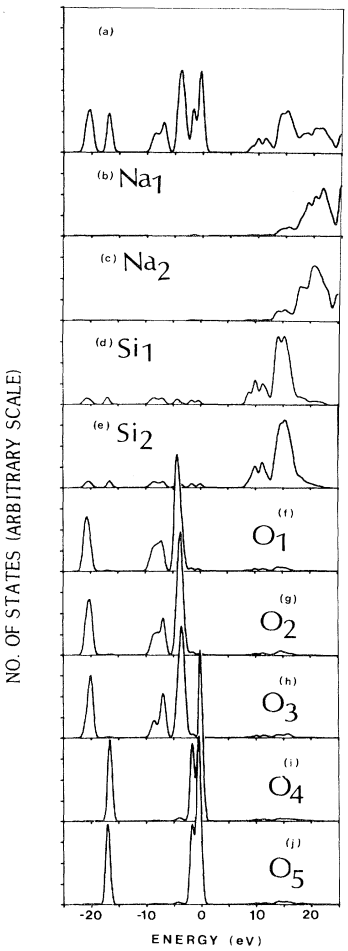

FIG. 10. Same as Fig. 9 for β-$Na_2Si_2O_5$. Calculated with $\alpha=1.0$.

would suggest that α should be approximately equal to 0.8. (The experimental splitting of the O 2s level is larger than the splitting at the O 1s level[2,14,15] and appears to be less sensitive to Na concentration.) Both the XPS data (O 2s splitting) and gap measurements favor a choice of $\alpha<1$. Unless explicitly stated, subsequent discussion will pertain to the $\alpha=\frac{2}{3}$ results.

For Na_2SiO_3, the O 2p band consists of a three-peak structure (peaks B_1,B_2,B_3 in Fig. 5) and the O 2s band is split (peaks A_1,A_2 in Fig. 5). The total DOS's for the α and β phase of $Na_2Si_2O_5$ are almost identical (see Figs. 6 and 7). The O 2p bands consist of 4 peaks (B_1,B_2,B_3,B_5) and a shoulder B_3', while the O 2s bands consist of two peaks A_2,A_3 and a shoulder A_1'. The position and their nature are summarized in Table III.

The details of the total DOS curves can be understood by studying the resolved components in terms of PDOS curves displayed on the lower panels of Figs. 5—10. Although the PDOS of NBO and BO are quite different with the former accounting for the sharp peak at the top of the VB, the PDOS for each type of O within different crystals are quite similar. Thus the calculated PDOS is sensitive to environmental difference between the two types of O atoms. Subtle differences in the spectra can be traced to slightly different bonding configurations (see Sec. II). For example, in the β-$Na_2Si_2O_3$ crystal, both O_4 and O_5 are NBO but their local environments are slightly different. Figure 7 indicates that O_4 has a dominant LDOS peak at -0.27 eV while O_5 peaks at -0.50 eV. This peak shift is a consequence of different mean Na-O distances. They are 2.435 Å for O_4 but 2.418 Å for O_5. The PDOS of all the NBO are quite similar with subtle differences controlled by the Si—O BL and the precise locations of nearby Na atoms. For BO O_1 of α-$Na_2Si_2O_5$, which has no nearby Na atoms, or for BO O_3 of β-$Na_2Si_2O_5$, which has one Na atom at the rather large distance of 2.495 Å, the BO PDOS resembles that of α-SiO_2 calculated using a similar approach.[16]

Sigel[11] found three peaks in the reflectance spectra of $(Na_2O)(SiO_2)_2$ and $(Na_2O)(SiO_2)_3$ glasses. The highest peak, which is also present in both crystalline and glassy SiO_2, occurs at 11.5 eV. The other two peaks are located at 8.5 and 9.3 eV. We suggest that the 11.5-eV peak is associated with transitions from occupied electron states represented in the most intense LDOS peak of the BO atoms to the extended and rather featureless empty conduction-band states. These initial BO states consist of nonbonding O 2p orbitals which are similar in both crystalline and vitreous SiO_2 and in the alkali silicates. The other two closely spaced reflectance peaks are probably associated with the two-peak structure in the PDOS of NBO. The weaker peak has been broadened into a shoulder in some PDOS curves in the $\alpha=\frac{2}{3}$ calculation, but is

TABLE III. DOS peak positions of three crystals in $\alpha=\frac{2}{3}$ calculation.

	Label	Peak position (eV)	Nature
Na_2SiO_3	A_1	−18.69	O_2, bridging, 2*s* orbitals
	A_2	−16.19	O_1, nonbridging, 2*s* orbitals
	B_1	−6.67	O_2, bridging 2*p* orbitals
	B_2	−3.27	
	B_3	−0.55	O_1, nonbridging, 2*p* orbitals
	C_1	15.10	Si and Na 3*s*-3*p* hybrid orbitals
α-$Na_2Si_2O_5$	A_1[a]	−18.63	O_2, bridging, 2*s* orbitals
	A_2	−17.65	O_1, bridging, 2*s* orbitals
	A_3	−16.14	O_3, nonbridging, 2*s* orbitals
	B_1	−7.75	O_1 and O_2 bridging 2*p* orbitals
	B_2	−5.71	
	B_3[a]	−2.31	O_2, bridging, 2*p* orbitals
	B_4	−1.85	O_1, bridging, 2*p* orbitals
	B_5	−0.27	O_3, nonbridging, 2*p* orbitals
	C_1	13.70	Si and Na 2*s*-3*p* hybrid orbitals
β-$Na_2Si_2O_5$	A_1[a]	−18.87	O_1, bridging, 2*s* orbitals
	A_2	−17.96	O_2 and O_3, bridging, 2*s* orbitals
	A_3	−16.15	O_4 and O_5 nonbridging, 2*s* orbitals
	B_1	−6.53	O_1, O_2, and O_3,
	B_2	−5.49	bridging,
	B_3	−2.99	2*p* orbitals
	B_4	1.63	
	B_5	−0.27	O_4 and O_5, nonbridging, 2*p* orbitals
	C_1	13.78	Si_1 and Si_2 and Na_1 and Na_2 3*s*-3*p* hybrid orbitals

[a]Shoulder, not peak.

quite prominent in the $\alpha=1$ calculation.

In Fig. 11, we reproduce XPS valence band (VB) spectra of $(Na_2O)_x(SiO_2)_{1-x}$ glasses with $x=0.0$, 0.22, 0.39, and 0.50. The spectra are scaled to maintain a constant Si 2*p* intensity. The Na 2*p* line appears near 28 eV. The O 2*s* level ($\sim$21 eV) is split into bridging and nonbridging components with the low binding energy NBO peak growing with increasing Na concentration. With increasing *x*, the intensity of the low BE side of the valence band also dramatically increases. This observation is consistent with the calculations of Figs. 5—10 which show that the dominant O 2*p* contribution from NBO always appears at lower binding energy than the O 2*p* associated with BO. This point was also noted in Ref. 17.

Figure 12 shows the calculated DOS for α-$Na_2Si_2O_5$ and Na_2SiO_3 compared with XPS data for samples with corresponding chemical compositions (Na 2*p* levels were not included in the calculations). The calculated results are convoluted with a 1.3-eV Gaussian, comparable to the apparent broadening of the XPS spectra. The more intense features of the DOS curve correspond well with the strong features of the XPS spectra. However, intensity variations between corresponding features of the calculated and measured spectra are severe. The experimental data are "distorted" by varying transitions probabilities

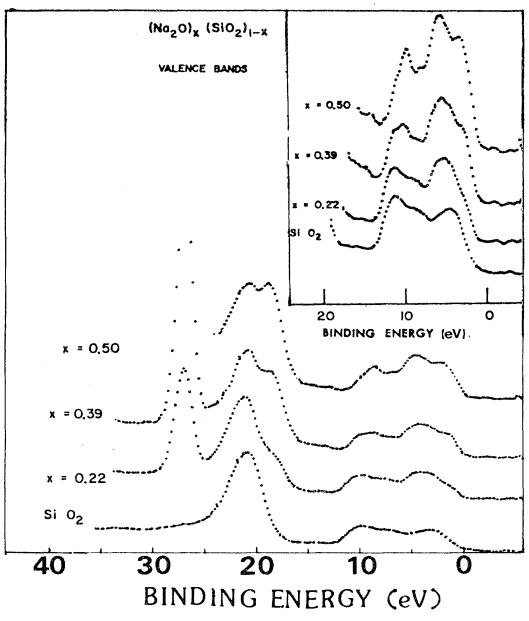

FIG. 11. XPS spectra for $(Na_2O)_x(SiO_2)_{1-x}$. The inset shows an enlargment of the VB region.

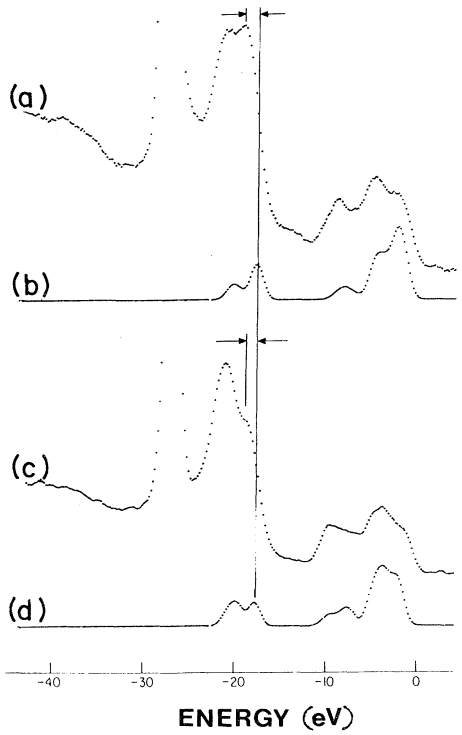

FIG. 12. (a) XPS spectra for Na_2SiO_3 glass compared with (b) DOS calculation; (c) XPS spectra for $Na_2Si_2O_5$ compared with (d) DOS calculation.

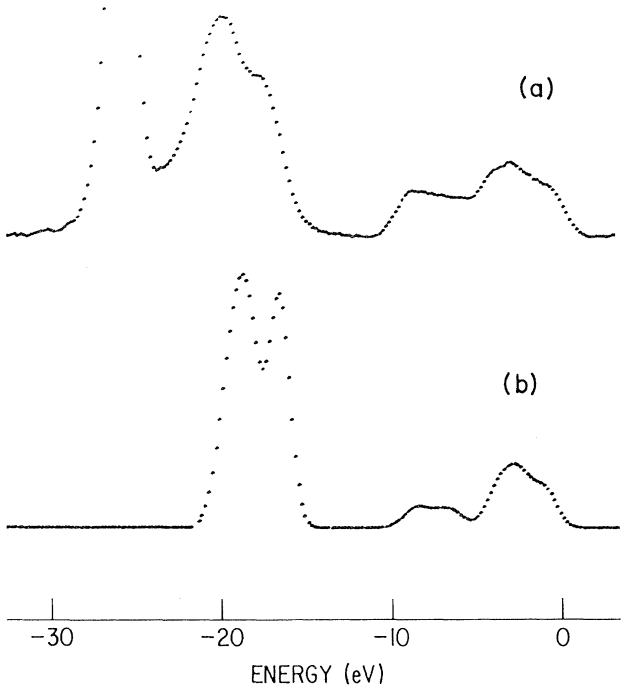

FIG. 13. (a) XPS spectra of $Na_2Si_2O_5$ compared with (b) DOS calculation. PDOS contributions were scaled to account for varying XPS transition probabilities and XPS data were corrected for inelastic loss.

associated with the different electron states excited in the measurement process.

We have attempted to account for these intensity variations by scaling the PDOS results using the atomic cross-section calculations of Scofield.[18] Relative scaling factors (per electron) from these calculations are as follows: O 2*s*, 14.6; O 2*p*, 1.0; Si 3*s*, 8.4; Si 3*p*, 1.5 for 1487-eV incident photons. The calculated PDOS curves contributed by each of these orbitals were separately scaled and the scaled contributions recombined. The results are shown in Fig. 13 (again convoluted with a 1.3-eV Gaussian) along with a $Na_2Si_2O_5$ XPS spectrum. A correction (of the XPS data) was made for inelastic electron loss by assuming that a constant (energy-independent) loss contribution, proportional to the signal intensity, occurs at each energy increment. Enlargements of the valence-band data for $Na_2Si_2O_5$ and for Na_2SiO_3 are shown in Fig. 14 compared with the calculated spectra obtained by incorporating the Scofield scaling factors. The correspondence between theory and experiment is now much improved. Some O 2*s* and Si 3*s* states, heavily weighted in the scaling process, occur near the bottom of the valence band. Scaling thus enhances this portion of the spectrum to produce improved agreement with experiment. The point being made in Fig. 13 is that the relative photoemission cross section of the different angular momentum components of the DOS are different. In consequence, the shape of experimental XPS DOS will be distorted relative to the general ground-state DOS calculation. By scaling the various components with Scofield factors, a correction is made for this effect. No reference is made to the absolute magnitude. Such scaling procedures have been used by other investigators to account for VB distortions.[19] In Fig. 15, both amorphous and crystalline $Na_2Si_2O_5$ XPS spectra are presented. Within resolution and random noise limitations, the glass and crystal spectra are identical (and are well represented by the theoretical curve). Thus it would appear that variations within the disilicate, in the conversion from crystal to glass, are rather subtle.

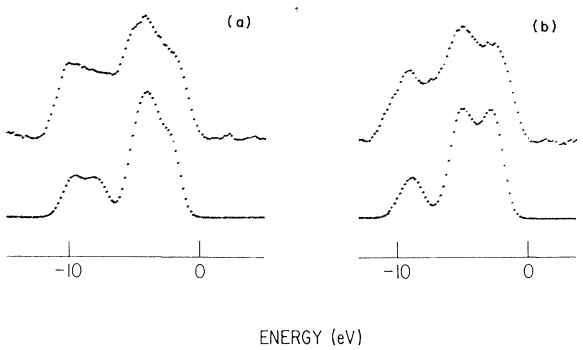

FIG. 14. Valence band XPS data (upper curve) for (a) $Na_2Si_2O_5$ and (b) Na_2SiO_3 compared with calculated spectra (lower curve) obtained by incorporating Scofield scaling of PDOS components.

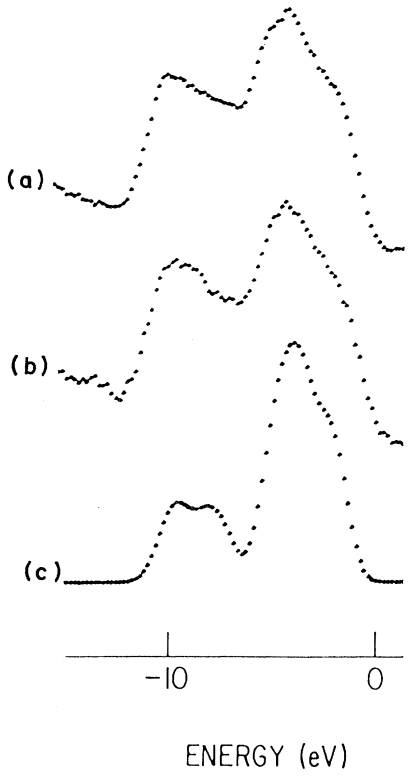

FIG. 15. XPS spectra for both (a) a crystalline and (b) amorphous $Na_2Si_2O_5$ sample compared with the scaled DOS calculation (c).

TABLE IV. Valence-electron distribution.

Crystal	Atom	$\alpha=\frac{2}{3}$	$\alpha=1.0$
Na_2SiO_3	Na	0	0
	Si	1.3	1.1
	O_1 (nonbridging)	7.6	7.7
	O_2 (bridging)	7.5	7.6
α-$Na_2Si_2O_5$	Na	0	0
	Si	1.1	1.0
	O_1 (bridging)	7.6	7.6
	O_2 (bridging)	7.6	7.6
	O_3 (nonbridging)	7.6	7.6
β-$Na_2Si_2O_5$	Na_1	0	0
	Na_2	0	0
	Si_1	1.2	1.1
	Si_2	1.1	1.1
	O_1 (bridging)	7.5	7.6
	O_2 (bridging)	7.6	7.6
	O_3 (bridging)	7.5	7.6
	O_4 (nonbridging)	7.6	7.6
	O_5 (nonbridging)	7.6	7.6
(a-SiO_2)[a]	Si	0.93	
	O	7.54	

[a]Reference 16.

The theoretical valence-band widths closely correspond to experiment. Some narrowing of the valence band is observed (both in XPS and DOS) as sodium content is increased. In Fig. 13, we also see that the position of the calculated O 2s levels is shifted by ~ 1 eV relative to experiment (with valence bands aligned). This shift may be a consequence of photoemission final-state effects. Final-state relaxation shifts at the relatively localized O 2s hole state may be somewhat different from the ground-state separation (represented in the DOS calculation).

C. Effective Charges

Effective charges on each atom for each crystal structure were calculated according to Mulliken's population analysis scheme[10] and are listed in Table IV. Such a scheme only provides approximate values of effective charge but works reasonably well when the basis functions are not too extended. We shall regard these effective charges as estimates suitable for qualitative comparisons. Based on the values listed in Table IV, we note the following points:

(i) The Na atoms give up their valence charge entirely and appear as bare positive ions. Furthermore, the Na ions in the crystals are positioned at approximately the same distance from BO as from NBO sites. Even though the Na atom gives up its charge to a nearby O atom (NBO), that Na atom is not held in closer proximity to the NBO than it is to other bridging O atoms. Apparently, Na^+ ions are only weakly bonded to identifiable crystallographic sites.

(ii) The Mulliken analysis shows only a small difference between the effective charges of BO and NBO (less than 0.1 electron). A similar type of model calculation for effective charges in α-SiO_2 gives average effective charges of 0.93 and 7.54 electrons on Si and O atoms, respectively,[16] approximately the values obtained here. These calculations would indicate, in replacing a silicon bond (Si—O—Si) with a Na bond (Si—O—Na), that very little net charge readjustment occurs at the oxygen site. This result is consistent with the observation that Si is also seen to be very ionic (~ 3 electrons transferred per Si atom) within the Mulliken scheme. Nonetheless, the electropositive Na atom is more able than Si to give up its charge to an oxygen atom (1.0 electron vs ~ 0.7 electrons per bond, respectively). Consequently, more charge (~ 0.1 electron) is found on NBO than BO. Even so, the Mulliken analysis probably underestimates the amount of charge differential between the NBO and BO. (The 2p wave functions at the O sites are spatially very extended, overlapping neighboring atoms so that the assignment of charge to a given oxygen site is somewhat ambiguous.) The effective charge differential between NBO and BO is more dramatically emphasized in XPS data. A large (~ 2 eV) relative shift in the binding energies of O 1s levels for NBO and BO is observed.[2,14,15] Furthermore, the separa-

tion between NBO and BO increases as the alkali becomes more electropositive (e.g., Cs silicate glasses show larger shifts than Li glasses).[14]

(iii) A secondary consequence of replacing a bridging oxygen by a nonbridging oxygen is that the oxygen outer shell is more easily filled (than by bonding exclusively to Si) so that the O atom can somewhat reduce its attraction for electrons from Si neighbors. Thus with this replacement, charge relaxes back to the Si sites. This charge readjustment is identified in the Mulliken analysis results of Table III, where we note that the charge on Si atoms in the Na "dilute" $Na_2O{\cdot}2SiO_2$ is less than the Si charge in the Na-rich $Na_2O{\cdot}SiO_2$ compounds. (In $Na_2O{\cdot}2SiO_2$ there is one NBO per SiO_4 tetrahedral unit and there are two NBO's per tetrahedron in $Na_2O{\cdot}SiO_2$.) This charge-relaxation effect was also noted in earlier XPS studies of alkali-silicate glasses.[2] With increasing Na concentration, Si core lines were observed to occur at lower binding energies, indicative of a more negatively charged local Si environment.

In studying charge distributions in the crystalline silicates, one cannot always associate a given Na ion with a particular NBO. The alkali ions may be distributed in the ordered lattice in such a way that the one-to-one correspondence cannot be recognized. Na ions even appear in close proximity to bridging oxygens. Nonetheless, the local environments of BO and NBO are substantially different. When Na_2O is added to silicates, charge supplied by the Na atom is predominately transferred to the NBO with some secondary charge redistribution among other members of the lattice.

V. CONCLUSIONS

We have made a comparative study of electronic structures of the crystalline phases of sodium metasilicate and α and β phase of sodium disilicates and have experimentally determined XPS spectra of $(Na_2O)_x(SiO_2)_{1-x}$ glasses. By careful analysis of local atomic environments in each crystal and by intercomparison of their electronic structures, we have examined the correlation between the electronic and atomic structures. We hold the view that, apart from the absence of long-range periodicity, local atomic environments of SiO_2 glasses containing Na_2O should be similar to those of crystalline sodium silicates. This view is supported by the observation that essentially identical XPS spectra were observed for both crystalline and amorphous $Na_2Si_2O_5$. Consequently, inferences pertaining to local charge distributions that are drawn from model calculations on appropriate crystals are also considered relevant to amorphous silicates. The calculated DOS for the three crystals studied agrees well with XPS measurements on alkali glasses (or crystals) of comparable compositions. It thus appears likely that a similar type of calculation on disordered glass systems $(Na_2O)_x(SiO_2)_{1-x}$ with comparable interatomic spacings will yield similar results for the effective charges. It is not clear, however, if sheetlike or chainlike structures with spacious channels such as those found in the crystalline metasilicate and disilicates, exist in glass systems. If so, what are the effects of such open channels on the electronic structure? It should be informative to examine, in the spirit of quasi-periodic models,[16] a variety of "realistic" structures for $(Na_2O)_x(SiO_2)_{1-x}$ glasses, using crystal information as a guideline for the short-range order. First-principles calculations of the electronic structure for such glass models can then be performed.

In the present first-principles, non-self-consistent, minimal basis calculations which use two different exchange potential models, the DOS results are quite similar and quite accurately correspond to XPS valence-band data. The results are encouraging and support the contention that the computational approach can be meaningfully utilized to study other highly complicated alkali-silicate crystals and glassy systems. A systematic microscopic understanding of the structures and properties of other alkali-silicate glasses, mixed alkali silicates as well as those involving transition-metal elements may be obtained.

ACKNOWLEDGMENT

Work at University of Missouri—Kansas City supported by U.S. Department of Energy Contract No. DE-AC02-79ER10462. Work at Argonne is supported by the U.S. Department of Energy Contract No. W31-109-ENG-38.

[1]See for example, J. Wong and C. A. Angell, *Glass Structure by Spectroscopy* (Marcel Dekker, New York, 1976).

[2]B. W. Veal and D. J. Lam in *Proceedings of International Conference on Physics of SiO_2 and its Interfaces*, edited by S. T. Pantelides (Pergamon, New York, 1978), p. 298.

[3]A. Grund and M. Pizy, Acta Crystallogr. 5, 837 (1952); W. S. McDonald and D. W. J. Cruickshank, *ibid.* 22, 37 (1967).

[4]A. K. Pant and D. W. J. Cruickshank, Acta Crystallogr. Sec. B 24, 13 (1968).

[5]A. Grund, Bull. Soc. Fr. Mineral. Cristallogr. 77, 775 (1954); A. K. Pant, Acta Cryst. Sec. B 24, 1077 (1968).

[6]W. Y. Ching and C. C. Lin, Phys. Rev. B 12, 5536 (1975); 16, 2989 (1977).

[7]E. E. Lafon and C. C. Lin, Phys. Rev. 152, 579 (1966); R. C. Chaney, T. K. Tung, C. C. Lin, and E. E. Lafon, J. Chem. Phys. 52, 361 (1970).

[8]S.-Y. Ren and W. Y. Ching, Phys. Rev. B 23, 5454 (1981); 24, 5788 (1981).

[9]J. C. Slater, Phys. Rev. 81, 385 (1951); R. Gaspar, Acta. Phys. Hung. 3, 263 (1954); W. Kohn and L. J. Sham, Phys. Rev. 140, A1133 (1965).

[10]R. S. Mulliken, J. Am. Chem. Soc. 77, 887 (1954).

[11]G. H. Sigel, J. Non-Cryst. Solids 13, 372 (1973/74).

[12]T. H. DiStefano and D. E. Eastman, Solid State Commun. 9, 2259, 1971.

[13]E. Ellis, D. W. Johnson, A. Breeze, D. M. Magee, and P. G. Perkins, Philos. Mag. B 40, (2), 105 (1979).

[14]R. Brückner, H.-U. Chun, H. Goretski, and M. Sammet, J.

Non-Cryst. Solids 42, 49 (1980).
[15]J. S. Jen and Kalinowski, J. Non-Cryst. Solids 38, 21 (1979).
[16]W. Y. Ching, Phys. Rev. Lett. 46, 607 (1981); Phys. Rev. B 26, 6622 (1982).
[17]D. J. Lam, A. P. Paulikas, and B. M. Veal, J. Non-Cryst. Solids 42, 41 (1980).
[18]J. H. Scofield, J. Electron Spectrosc. Relat. Phenom. 8, 129 (1976).
[19]See for example, G. K. Wertheim, L. F. Mattheiss, M. Campagna, and T. P. Pearsall, Phys. Rev. Lett. 32, 997 (1974).